

Accepted Manuscript

6-Oxooxazolidine-quinazolines as noncovalent inhibitors with the potential to target mutant forms of EGFR

Jiaan Shao, En Chen, Ke Shu, Wenteng Chen, Guolin Zhang, Yongping Yu

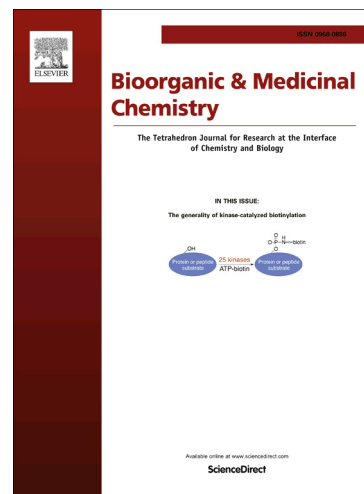
PII: S0968-0896(16)30289-9
DOI: <http://dx.doi.org/10.1016/j.bmc.2016.04.046>
Reference: BMC 12961

To appear in: *Bioorganic & Medicinal Chemistry*

Received Date: 24 March 2016
Revised Date: 21 April 2016
Accepted Date: 22 April 2016

Please cite this article as: Shao, J., Chen, E., Shu, K., Chen, W., Zhang, G., Yu, Y., 6-Oxooxazolidine-quinazolines as noncovalent inhibitors with the potential to target mutant forms of EGFR, *Bioorganic & Medicinal Chemistry* (2016), doi: <http://dx.doi.org/10.1016/j.bmc.2016.04.046>

This is a PDF file of an unedited manuscript that has been accepted for publication. As a service to our customers we are providing this early version of the manuscript. The manuscript will undergo copyediting, typesetting, and review of the resulting proof before it is published in its final form. Please note that during the production process errors may be discovered which could affect the content, and all legal disclaimers that apply to the journal pertain.

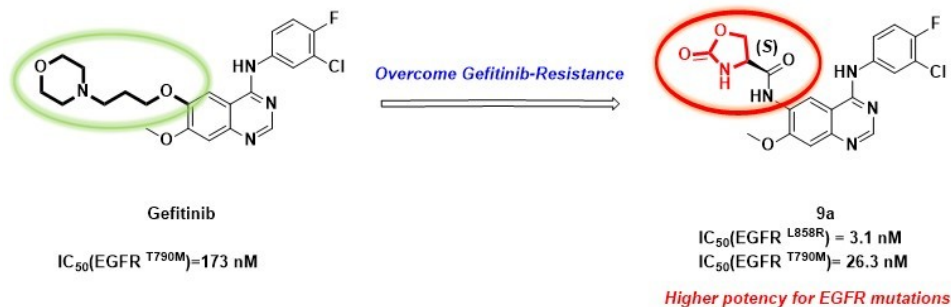


Graphical Abstract

6-Oxooxazolidine-quinazolines as noncovalent inhibitors with the potential to target mutant forms of EGFR

Leave this area blank for abstract info.

Jiaan Shao, En Chen, Ke Shu, Wenteng Chen, * Guolin Zhang, * Yongping Yu*
Zhejiang Province Key Laboratory of Anti-Cancer Drug Research, College of Pharmaceutical Science,
Zhejiang University, Hangzhou 310058, P. R. China





6-Oxooxazolidine-quinazolines as noncovalent inhibitors with the potential to target mutant forms of EGFR

 Jiaan Shao,^a En Chen,^a Ke Shu,^a Wenteng Chen,^{*,a} Guolin Zhang,^{*,a} Yongping Yu,^{*,a}
^a Zhejiang Province Key Laboratory of Anti-Cancer Drug Research, College of Pharmaceutical Science, Zhejiang University, Hangzhou 310058, P. R. China

ARTICLE INFO

Article history:

 Received
 Received in revised form
 Accepted
 Available online

Keywords:

 Drug resistance
 Noncovalent EGFR inhibitors
 Oxooxazolidine
 Quinazoline
 Hybrids

ABSTRACT

Despite the remarkable benefits of gefitinib, the clinical efficacy is eventually diminished due to the acquired point mutations in the EGFR (T790M). To address this unmet medical need, we demonstrated a strategy to prepare a hybrid analogue consisting of the oxooxazolidine ring and the quinazoline scaffold and provided alternative noncovalent inhibitors targeting mutant forms of EGFR. Most of the derivatives displayed moderate to good anti-proliferative activity against gefitinib-resistant NCI-H1975. Some of them exhibited potent EGFR kinase inhibitory activities, especially on EGFR^{T790M} and EGFR^{L858R} kinases. SAR studies led to the identification of a hit **9a** that can target both of the most common EGFR mutants: L858R and T790M. Also, **9a** displayed weaker inhibitory against cancer cell lines with low level of EGFR expression and good chemical stability under different pH conditions. The work presented herein showed the potential for developing noncovalent inhibitors targeting EGFR mutants.

2009 Elsevier Ltd. All rights reserved.

1. Introduction

Lung cancer has become the leading cause of cancer-related deaths worldwide.^[1] More than 80% of lung cancers are identified as non-small-cell lung cancer (NSCLC) with a 5-year survival rate of less than 1%.^[2] Genetic aberration in the epidermal growth factor receptor has been well-validated as one of key drivers of NSCLC progression.^[3-4] The FDA approval of gefitinib and erlotinib shows a significant benefit for NSCLC patients with EGFR-activating mutations, namely, exon 19 deletion or L858R mutations.^[5-6] Though such TK inhibitors have gained the role in the treatment of NSCLC, the short-lived clinical outcome develops after months of treatment. The EGFR T790M mutation in exon 20 is the most common cause of acquired resistance, accounting for about 50% of cases.^[7] EGFR with L858R/T790M mutations greatly increases the affinity for ATP, thus reducing the potency of ATP-competitive kinase inhibitors.^[8]

The predominant strategy to combat the resistance has been the use of covalent inhibitors, increasing target residence time and providing strong potency. For this reason, second- and third-generation EGFR inhibitors, including afatinib,^[9] CO-1686^[10]

and AZD9291^[11] have been designed to form a covalent bond with Cys797 showing promising efficacy. However, recent reports have been demonstrated that the new acquired C797S mutations are associated with resistance to EGFR irreversible inhibitors in NSCLC.^[12] These findings indicate that drugs owning excellent potency on EGFR without relying on the covalent modification of C797 are in demand. Herein, our work focuses on developing alternative noncovalent strategy that provides new inhibitors with the potency to overcome the problem of gefitinib-resistance. It will also provide chemical starting points for optimization of the efficacy/toxicity ratio.

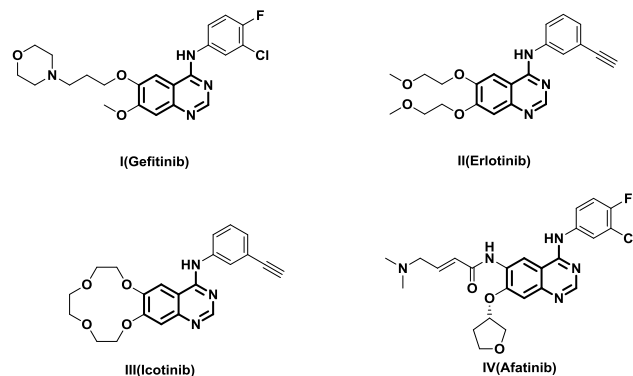


Figure 1. The representative clinical EGFR-TK inhibitors based on the quinazoline scaffold

*corresponding authors

Email address: wentengchen@zju.edu.cn (W. Chen)
guolinzhang@zju.edu.cn (G. Zhang)
yyu@zju.edu.cn (Y. Yu)

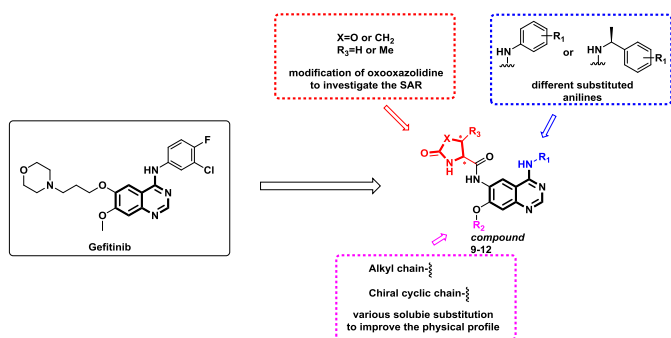
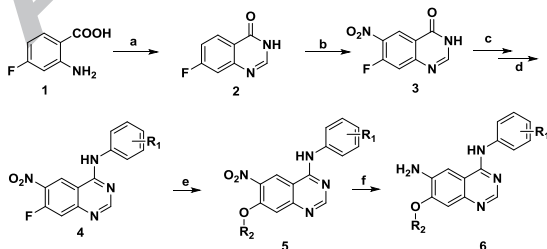


Figure 2. Design strategy for 6-oxooxazolidine-quinazoline hybrids **9-12**

With the purpose of developing a novel noncovalent strategy, a heterocycle ring was introduced into the 6-position of quinazoline ring on the basis of triggering additional hydrogen bonding interaction with mutant EGFR kinases. And then further focal point was centered on the 4-anilino moiety, 7-substituents and the modification of oxooxazolidine rings to investigate the structure-activity relationship (SAR). In this end, novel quinazoline analogues with the fine-tuned oxooxazolidine ring were synthesized. Their *in vitro* antiproliferative effects against gefitinib-sensitive human epithelial cancer cell A431, gefitinib-resistant NCI-H1975 and EGFR-independent cancer cell lines were assessed. Additionally their EGFR mutant kinase inhibitory activities as well as EGFR autophosphorylation inhibition were evaluated. Among these designed compounds, it is remarkably inspiring that the compound **9a** showed as the most potent compound against NCI-H1975 and mutant EGFR kinases, indicating the potential for overcoming the gefitinib-resistance.

2. Chemistry

The synthesis of the anilinoquinazolines **6** is depicted in **Scheme 1**. Briefly, 2-amino-4-fluorobenzoic acid **1** was converted to the quinazolinone **6** in 50% yield in six steps according to the reported procedure.^[13] The reaction sequence was initiated using commercially available 2-amino-4-fluorobenzoic acid **1** and formamidin acetate in 2-methoxyethanol at reflux to yield 7-fluoroquinazolin-4(3*H*)-one **2**, which was nitrified with concentrated H₂SO₄ and fuming HNO₃. The resulting 7-fluoro-6-nitro-3*H*-quinazolin-4-one **3** was chlorinated with excessive thionyl chloride in the presence of a catalytic amount of DMF for the preparation of 4-chloroquinazoline with subsequent aniline substitution to provide 4-anilino-7-fluoro-6-nitroquinazoline **4**. The fluorine atom was substituted by a variety of alcohols using *t*-BuOK in DMSO yielding the intermediate **5**. Reduction of the 6-nitro group with NaBH₄ and NiCl₂·H₂O in methanol gave the desired product **6**.

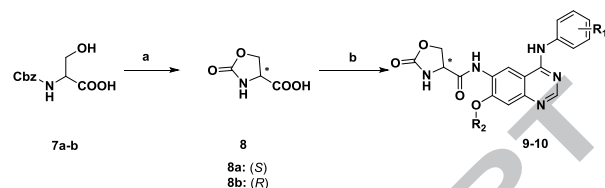


Reagents and conditions: a) formamidin acetate, 2-methoxyethanol, reflux, 18 h; b) HNO₃, H₂SO₄, 110 °C, 2 h; c) SOCl₂, DMF, reflux, 4 h; d) aniline, DCM, rt, 30 min; e) aliphatic alcohol, *t*-BuOK, DMSO, rt, 30 min; f) NaBH₄, SnCl₂·6H₂O, DCM-MeOH, ice-bath, 30 min;

Scheme 1. Synthesis of the compounds **6**

Various oxooxazolidine carboxylic acid groups, such as compounds **8a-d** were synthesized^[14] and incorporated into the

6-position of the anilinoquinazoline **6** via amide bond formation to give the corresponding compounds **9-12** (**Schemes 2** and **3**). The purities of all compounds were evaluated by HPLC-MS. The stereocenter of the products was not affected during the synthesis procedure according to the reported.^[14]

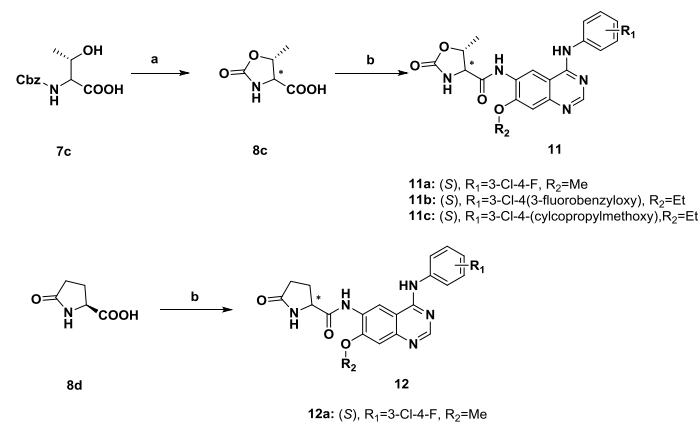
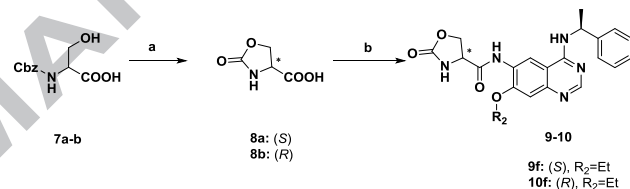


9a: (S), R₁=3-Cl-4-F, R₂=Me
9b: (S), R₁=3-Cl-4-(3-fluorobenzyloxy), R₂=Et
9c: (S), R₁=3-Br, R₂=Me
9d: (S), R₁=3-Cl-4, R₂=Me
9e: (S), R₁=3-Cl-4-(pyridin-2-ylmethoxy), R₂=Et
9g: (S), R₁=3-(3-fluorobenzyloxy)-1*H*-indazol-5-yl, R₂=Et
9h: (S), R₁=3-Cl-4-(6-methylpyridin-3-yl)oxy, R₂=Et
9i: (S), R₁=3-Cl-4-cyclopropylmethoxy, R₂=Et
9j: (S), R₁=4-methoxy, R₂=Me
9k: (S), R₁=3-Cl-4-F, R₂=(S)-tetrahydrofuran-3-yl
9l: (S), R₁=3-Cl-4-F, R₂=(S)-1-methylpiperidin-4-ylmethyl
9m: (S), R₁=3-Cl-4-F, R₂=(1-methylpiperidin-4-yl)methyl
9n: (S), R₁=3-Cl-4-F, R₂=2,2,2-trifluoroethyl
9o: (S), R₁=3-Cl-4-F, R₂=(*R*)-4-methylmorpholin-3-ylmethyl
9p: (S), R₁=3-Cl-4-F, R₂=2-methoxyethyl
9q: (S), R₁=3-Cl-4-F, R₂=2-(piperidin-1-yl)ethyl
9r: (S), R₁=3-Cl-4-F, R₂=3-morpholinopropyl

10a: (R), R₁=3-Cl-4-F, R₂=Me
10b: (R), R₁=3-Cl-4-(3-fluorobenzyloxy), R₂=Et
10c: (R), R₁=3-Br, R₂=Me
10e: (R), R₁=3-Cl-4-(pyridin-2-ylmethoxy), R₂=Et
10g: (R), R₁=3-(3-fluorobenzyloxy)-1*H*-indazol-5-yl, R₂=Et
10h: (R), R₁=3-Cl-4-F, R₂=(S)-tetrahydrofuran-3-yl
10i: (R), R₁=3-Cl-4-F, R₂=(1-methylpiperidin-4-yl)methyl
10j: (R), R₁=3-Cl-4-F, R₂=2-methoxyethyl
10l: (R), R₁=3-Cl-4-F, R₂=3-morpholinopropyl

Reagents and conditions: a) NaOH-H₂O, 0 °C-rt; b) compound **6**, (COCl)₂, Et₃N, DMF, DCM, ice-bath to rt, overnight

Scheme 2. Synthesis of the compounds **9-10**



Reagents and conditions: a) NaOH-H₂O, 0 °C-rt; b) compound **6**, (COCl)₂, Et₃N, DMF, DCM, ice-bath to rt, overnight

Scheme 3. Synthesis of the compounds **9-12**

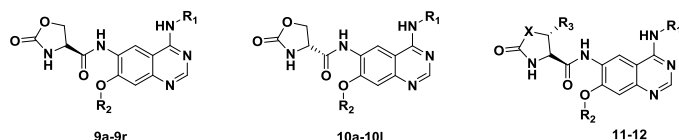
3. Results and discussion

3.1. In vitro anti-proliferative activity

To assess the potency for EGFR inhibitory activity, the 6-oxooxazolidine-quinazoline hybrids were tested against various cancer cells, including human epithelial carcinoma cell A431 overexpressing wild-type EGFR and gefitinib-resistant NSCLC cell H1975 possessing L858R/T790M mutant EGFR. As shown in **Table 1**, some of them displayed higher antiproliferative activity on H1975 cells (IC₅₀ = 3.87-9.33 μM) than gefitinib (IC₅₀ = 14.38 μM). **Table 1** also summarizes the SAR of these hybrids. The IC₅₀ values of the enantiomers showed that the stereochemistry has no significant effect on antiproliferative inhibitory. (For example **9a** vs **10a**, **9b** vs **10b**, and **9c** vs **10c**)

Notably, compound **9a** with a 3-chloro-4-fluoroaniline moiety to the position 4 was more potent against NCI-H1975 compared to the 3-bromo (**9c**) and 3-trifluoromethyl (**9d**) aniline. This effect was even more pronounced with placing large lipophilic groups at the *para* position of the 4-anilino substituent, such as 3-fluorobenzoyloxy group (**9b**) or cyclopropylmethoxy group (**9i**), whereas a (3-fluorobenzyl)-1*H*-indazol-5-yl (**9g**) or pyridin-2-methoxy (**9e**) substituent would lead to a decreased or even a loss of antiproliferative activities.

Table 1. Antiproliferative activities of compounds **9-12** against cells harboring different status of EGFR



No.	IC ₅₀ / μM ^a	
	A431 ^b	NCI-H1975 ^c
9a	9.20	6.80
10a	16.80	21.17
9b	3.89	3.87
10b	4.15	4.75
9c	7.25	9.08
10c	14.30	11.11
9d	13.50	10.84
9e	>50	23.3
10e	>50	>50
9f	16.90	15.34
10f	15.00	4.95
9g	10.75	10.54
10g	18.90	>50.0
9h	11.25	7.65
9i	5.05	5.08
9j	34.85	10.00
9k	22.75	9.33
10h	11.00	>50.0
9l	12.60	13.60
9m	2.43	21.1
10i	5.30	13.46
9n	33.90	>50
9o	18.65	7.40
9p	25.85	22.06
10j	>50.0	>50.0
9q	3.50	5.85
9r	48.7	12.3
10l	>50.0	37.2
11a	8.65	8.98
11b	3.36	4.28
11c	7.35	12.70
12a	21.80	>50
Gefitinib	4.58	14.38

^a The inhibitory effects of individual compounds on the proliferation of cancer cell lines were determined by the MTT assay. The data reported are the mean values from three independent experiments. ^b A431 is human epithelial carcinoma cell line (EGFR^{WT}). ^c H1975 is a human non-small-cell lung cancer cell line (EGFR^{L858R/T790M}).

Among the compounds tested, we found that the replacement of the aromatic ring with a chiral phenylethanol side chain (**9f**) maintained the potency against both cancer cell lines. The side chains at the 7-position of the quinazolinone core were also explored (**Table 1**). When the methoxyl group (**9a**) was replaced

with other alkyl side chains, such as trifluoroethoxyl (**9n**) or 2-methoxyethoxyl (**9p**), the resulting compounds showed less potency against A431 and NCI-H1975. Some other cyclic substituents (for example **9k**, **9l**, **9m**, **9o**, **9r**) incorporated into the 7-position exhibited moderate antiproliferative potency. Whereas, the derivative **9q** bearing a 2-(piperidin-1-yl) ethoxyl group was much more potent against the two cancer cell lines with IC₅₀ values of 3.50 μM (A431) and 5.85 μM (NCI-H1975), respectively. As shown in **Table 1**, compounds **11a-11c** with a chiral (*R*)-methyl branch at the 2-position of the oxazolidinone ring displayed similar activities compared to the parent counterparts. Finally, introducing a pyrrolidin-2-one group (**12a**) results in a significant loss of potency against both cancer cell lines.

3.2. EGFR kinase inhibitory assay

The inhibitory activities of the selected compounds against different types of kinases (EGFR^{WT}, EGFR^{L858R}, and EGFR^{T790M}) were evaluated using Homogeneous time-resolved fluorescence (HTRF) method, and gefitinib was employed as positive controls (**Table 2**). Among the tested compounds, some exhibited more potent than gefitinib, especially on EGFR^{T790M}. Notably, compounds **9a**, **9r** and **11a** (IC₅₀ < 100 nM) with a 3-chloro-4-fluoro anilino moiety at the 4-position of quinazolinone ring displayed higher inhibitory activity on EGFR^{T790M} than gefitinib (IC₅₀ = 173 nM). While the replacement of aniline with chiral alkyl amine (**9f**) led to a loss in inhibitory activity (for EGFR^{T790M}, IC₅₀ > 1000 nM). And the bulky substituents (compounds **9b**, **10b** and **11b**) at the 4-position was not favor leading a 2~5 fold decrease on the EGFR^{T790M} inhibitory activity. Among them, the most potent compound **9a** exhibited excellent inhibition against EGFR^{L858R} and EGFR^{T790M} with an IC₅₀ at 0.31 nM and 26.33 nM, respectively.

Table 2. Inhibitory activity of selected compounds against different types of EGFRs *in vitro*

Compound	EGFR IC ₅₀ / nM ^a		
	WT	L858R	T790M
9a	1.06	0.31	26.33
9b	1.34	5.62	53.16
9c	0.47	0.38	126.30
9f	5.52	0.71	>1000
9i	37.81	52.08	80.84
9q	25.53	7.79	332.60
9r	4.54	0.83	58.73
10b	1.19	5.49	110.60
11a	1.98	0.35	40.16
11b	2.57	12.00	294.60
Gefitinib	76.0	/	173.0

^aEGFR activity assays were performed using HTRF method. The data reported are the mean values from three independent experiments.

3.3 *In vitro* cytotoxicity assay

Since EGFR is expressing in many tissues for normal cellular processes, the potential for the toxicity from EGFR inhibitors is a concern. Therefore, the growth inhibitory of the compounds against cancer cell lines with low level of EGFR expression was evaluated to assess the potential non-specific toxicity. The cancer cell lines A549 and HepG2 express low levels of EGFR and therefore are good counter-screen cell lines for EGFR-targeting inhibitors. As shown in **Table 3**, all the tested compounds displayed weaker inhibitory than those against A431 and NCI-H1975. The results indicate that the non-specific cytotoxic effects of this hybrid are minimal.

Table 3. The inhibitory activities of compounds **9-11** against some cancer cell lines that express low levels of EGFR

Compound	IC ₅₀ / μM ^a	
	A549 ^b	HepG2 ^c
9a	14.93	>100
9b	11.60	>50.0
9c	>50.0	>100
9i	28.85	>100
9q	42.86	>50.0
10b	>50.0	>100
11a	>50.0	>50.0
11b	32.90	30.84
Gefitinib	>10.0	>50.0

^a The inhibitory effects of individual compounds on the proliferation of cancer cell lines were determined by the MTT assay. The data reported are the mean values from three independent experiments. ^b A549 is a human lung cancer cell line (EGFR WT/ κ -Ras dependent). ^c HepG2 is a human hepatic cancer cell line (EGFR-independent).

3.3 The mode of conjugation with GSH in solution

While previous work showed that the oxooxazolidine ring could undergo base-promoted sulfa-Michael additions with SH of cysteine [15], the chemical reactivity of this ring pendent on a 4-anilinoquinazoline scaffold remained speculative. Also, it is generally accepted that high reactivity towards glutathione (GSH) is associated with the risk of reactive metabolite formation. To address these issues, a representative compound **9a** was evaluated for the chemical reactivity toward low molecular weight (LMW) thiol nucleophile (reduced GSH) (Figure 3).

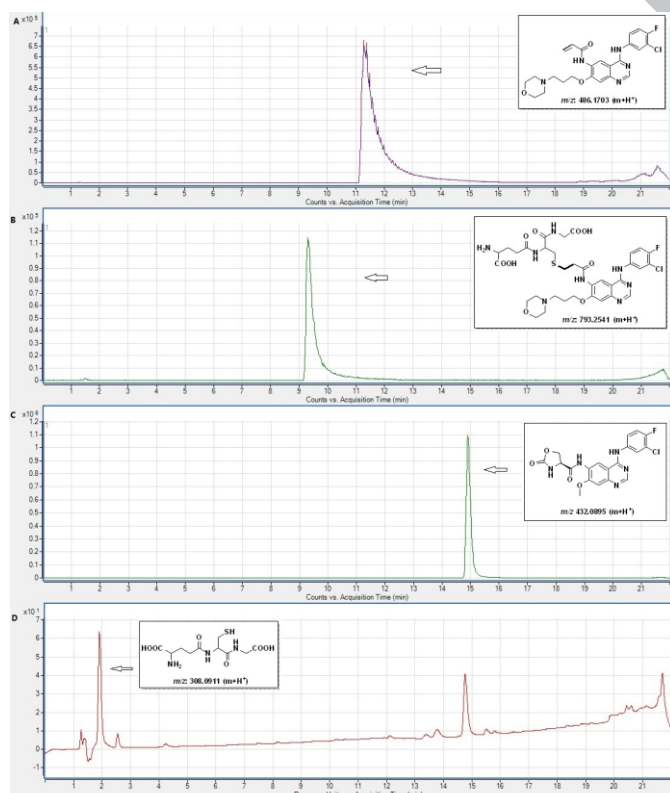


Figure 3. HPLC-HRMS chromatograms after a period of time of incubation in the presence of GSH (5 mM) and compound **9a** or canertinib (50 μM). A: canertinib, B: canertinib+GSH, t = 1440 min; C: compound **9a**; D: compound **9a**+GSH, t = 1440 min.

Compound **9a** and canertinib were reacted separately with 100 equivalents of GSH under physiological conditions for 1440 min and the reactions were monitored by HPLC-HRMS. In

comparison to canertinib, compound **9a** failed to form the corresponding adduct in 1440 min (compared to canertinib: 100%). These findings revealed that the oxooxazolidine ring has minimal propensity for covalent modification of Cys797 and minimal metabolic toxicity.

3.5 Inhibition of the EGF-induced phosphorylation of EGFR

To better understand the binding mode of this hybrid with EGFR kinase, **9a** was selected to inhibit the phosphorylation of EGFR in a no wash (left) and a wash out (right) experiment (Figure 4). The findings showed that **9a** inhibited EGFR phosphorylation in no wash experiment but not in the wash out. The results indicate that **9a** is acting through a reversible binding mode, suggesting **9a** is acting differently from the irreversible inhibitor canertinib.

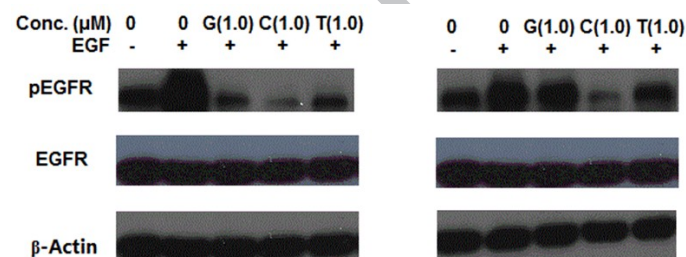


Figure 4. Inhibition of EGFR autophosphorylation in A431 by western blot assay. G: gefitinib, C: canertinib, T: compound **9a**

3.6 Stability study of compound 9a

Given the potent inhibition of EGFR mutant kinases and gefitinib-resistant NCI-H1975, together with the weaker inhibitory activity against other types of cancer cell lines (A549 and HepG2), the hit **9a** was chosen as the prototype of this hybrid and tested for its stability in buffered solutions at pH 7.4, 9.0 and 10.0 (Table 4).

9a was stable at pH 7.4 with percentage of remaining compound over 97% after 24 h of incubation at 37 °C in buffer. Under alkaline pH conditions (pH 9.0 and pH 10.0), **9a** showed high stability and was stable over the entire incubation time.

Table 4. *In vitro* stability studies on compound **9a**^a

Conditions	Percentage of compound 9a remaining (1 μM , 24 h)
pH 7.4	97.1%
pH 9.0	89.9%
pH 10.0	85.8%

^a Percentage of parent compound detected by HPLC-HRMS after incubation for the indicated time at 37 °C (see the experimental section)

3.7 Molecular docking study

To better understand how the oxazolidinone ring contributed to the EGFR kinase inhibitory activities, molecular docking was undertaken using Tripos Sybyl x1.3 molecular modeling package. [16] The co-crystal structure of EGFR^{T790M} in complex with afatinib was obtained from the RSC Protein Data Bank (PDB code: 4G5P).

Compound **9a** was initially docked to the EGFR active site cavity based on the structure of the Afatinib-EGFR^{T790M} complex and the resulting structure of the active site was shown in Figure 5.

It was found that **9a** forms hydrogen binding interactions in the hinge region between the N1 nitrogen and the backbone NH of Met 793. The aniline group at the 4-position of **9a** is located in a hydrophobic pocket, which is similar to afatinib. The docking studies also revealed that the NH of oxooxazolidine ring is oriented towards the O of Asp800, a weak hydrogen bond acceptor within a hydrogen bonding distance of 2.6 Å. The new interaction mode offers an explanation of the good potency against EGFR kinases (**Figure 5**).

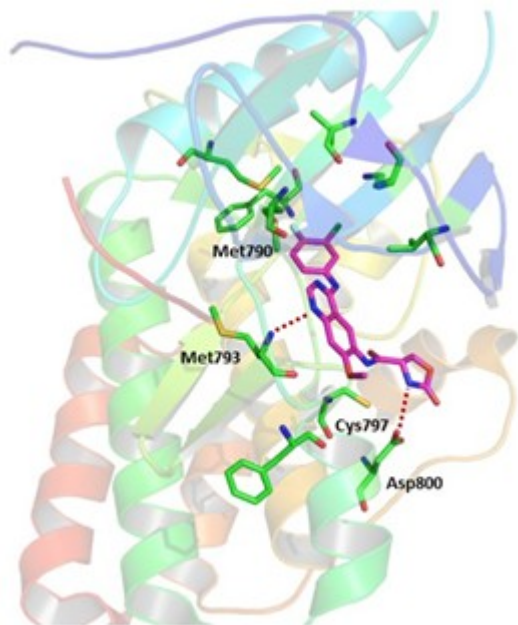


Figure 5. Putative binding mode of compound **9a** within the active pocket of the EGFR^{T790M} (PDB: 4G5P)

4. Conclusion

In summary, 6-oxooxazolidine-quinazoline hybrids were synthesized and subjected to pharmacological evaluation. The results showed that most of the derivatives possessed moderate to high potencies against gefitinib-sensitive cancer cell A431 and gefitinib-resistant cancer cell NCI-H1975. An EGFR kinase inhibition assay indicated that some of the tested derivatives displayed good inhibition against EGFR^{T790M}. The hit **9a** exhibited potent inhibition of L858R and T790M mutant EGFR and gefitinib-resistant cell line NCI-H1975. Additionally, **9a** displayed weaker inhibitory against several cancer cells with low level of EGFR expression as well as minimal chemical reactivity toward low molecular weight (LMW) thiol nucleophiles. These results demonstrated that the inherent non-specific toxicity of this hybrid may be minimal. Further studies showed that **9a** possessed good chemical stability under different pH conditions and reversibly inhibited EGF mediated phosphorylation of EGFR in A431 cell. These findings presented herein show the noncovalent inhibitor **9a** has the potential to targeting EGFR mutants.

5. Experimental

5.1 General Methods

Unless otherwise noted, all solvents and chemicals were used as purchased without further purification. Purity of all final compounds was 95% or higher. All reported yields are isolated yields after column chromatography. ¹H NMR spectra were recorded on a Bruker DRX-500 [Bruker Biospin, Germany].

Chemical shifts are reported in ppm relative to the residual solvent peak (CDCl₃, TMS: 0.00). Multiplicity was indicated as follows: s (singlet); d (doublet); t (triplet); q (quartet); m (multiplet); dd (doublet of doublet); dt (triplet of doublet); td (doublet of triplet); brs (broad singlet) etc. Intermediates were purified by column chromatography on silica gel (200-300 mesh). HPLC analysis and the HRMS of all biologically evaluated compounds was confirmed on a Agilent 1290 HPLC-6224 Time of Flight Mass Spectrometer using Phenomenex Luna 5μ C18, 100 Å, 150 X 4.60 mm 5 micron column at a flow rate of 0.5 mL/min using linear gradients buffer B in A (B: CH₃OH containing 0.1 % formic acid, A: H₂O containing 0.1% formic acid). Mobile phase B was increased linearly from 5% to 95% over 7 min and 95% over the next 2 min, after which the column was equilibrated to 5% for 1 min.

5.2 Synthesis of intermediates and target compounds

5.2.1 Representative intermediates:

7-Fluoro-3*H*-quinazolin-4-one (**2**).

A mixture of 2-amino-4-fluorobenzoic acid (126 g, 0.82 mol) and formamidine acetate (170 g, 1.64 mol) in 2-methoxyethanol (800 mL) was heated under reflux for 18 h, and the solution was concentrated. The residue was diluted with water, and the suspension was filtered, washed with water, and dried to give pure product (yield 88%). mp 235-237 °C. ¹H NMR (500 MHz, DMSO) δ 12.37 (s, 1H), 8.19 (dd, *J* = 8.5, 6.5 Hz, 1H), 8.15 (s, 1H), 7.46 (dd, *J* = 10.0, 2.5 Hz, 1H), 7.40 (td, *J* = 9.0, 2.5 Hz, 1H). HRMS (ESI): *m/z* calcd for (C₈H₅FN₂O+H)⁺:165.0464; found:165.0459.

7-Fluoro-6-nitro-3*H*-quinazolin-4-one (**3**).

7-Fluoro-3*H*-quinazolin-4-one (47.4 g, 0.29 mmol) was added to a mixture of concentrated sulfuric acid (100 mL) and fuming nitric acid (105 mL) at 0 °C. The resulting mixture was heated at 110 °C for 2 h. The solution was cooled to room temperature, then poured onto ice-water (1.5 L) to give a mixture of 6- and 8-nitroquinazolin-4(3*H*)-ones. Recrystallization from AcOH gave pure 7-fluoro-6-nitroquinazolin-4(3*H*)-one (yield 53%): mp 283-285 °C. ¹H NMR (500 MHz, DMSO) δ 12.81 (s, 1H), 8.71 (d, *J* = 8.5 Hz, 1H), 8.32 (s, 1H), 7.77 (d, *J* = 12.0 Hz, 1H). HRMS (ESI): *m/z* calcd for (C₈H₄FN₃O₃+H)⁺:210.0315; found:210.0312.

4-Chloro-7-fluoro-6-nitro-quinazoline and *N*-(3-chloro-4-fluorophenyl)-7-fluoro-6-nitroquinazolin-4-amine (**4-a**).

A suspension of 7-fluoro-6-nitro-3*H*-quinazolin-4-one (10.45 g, 50 mmol) in SOCl₂ (200 mL) containing 3 drops of DMF was heated under reflux for 4 h to give a clear solution. The SOCl₂ was removed under reduced pressure to give crude 4-chloro-7-fluoro-6-nitroquinazoline, which was used directly. The crude chloro-substituted compound was dissolved in 200 mL of CH₂Cl₂, and a solution of aniline (7.97 g, 55 mmol) in EtOH 50 mL was added. The resulting mixture was stirred at room temperature for 15 min when a precipitate of product hydrochloride formed. After a further 15 min sufficient hexane was added to ensure complete precipitation, and the solid was collected by filtration, washed with petroleum ether, and dried to give pure product (yield 95%). m.p.: 262-263 °C. ¹H NMR (500 MHz, DMSO) δ 11.85 (s, 1H), 9.90 (d, *J* = 7.5 Hz, 1H), 8.94 (s, 1H), 8.09 (dd, *J* = 9.0 Hz, 1H), 8.00 (d, *J* = 11.5 Hz, 1H), 7.81-7.78 (m, 1H), 7.55 (t, *J* = 9.0 Hz, 1H). HRMS (ESI): *m/z* calcd for (C₁₄H₇ClF₂N₄O₂+H)⁺:337.0304; found:337.0292.

(*S*)-*N*-(3-chloro-4-fluorophenyl)-6-nitro-7-((tetrahydrofuran-3-yl)oxy)quinazolin-4-amine (**5-a**).

To a suspension of *N*-(3-chloro-4-fluorophenyl)-7-fluoro-6-nitroquinazolin-4-amine (1.68 g, 5 mmol) and (*S*)-tetrahydrofuran-3-ol (0.66 g, 7.5 mmol) in DMSO (10 mL) at 25 °C was added *t*-BuOK (1.68 g, 15 mmol). After a further 30 min reaction, sufficient water was added to ensure complete precipitation, and the solid was collected by filtration, washed by water twice and dried to give the pure yellow solid. (yield 90%). m.p.: 221-223 °C; ¹H NMR (500 MHz, DMSO) δ 10.18 (s, 1H), 9.23 (s, 1H), 8.69 (s, 1H), 8.17 (dd, *J* = 6.5, 2.5 Hz, 1H), 7.82-7.79 (m, 1H), 7.50-7.46 (m, 2H), 5.46 (t, *J* = 5.5 Hz, 1H), 3.98 (dd, *J* = 10.5, 4.5 Hz, 1H), 3.92-3.84 (m, 2H), 3.83-3.78 (m, 1H), 2.39-2.32 (m, 1H), 2.10-2.05 (m, 1H); HRMS (ESI): *m/z* calcd for (C₁₈H₁₄ClFN₄O₄+H)⁺: 405.0766; found: 405.0775.

(*S*)-*N*-(3-chloro-4-fluorophenyl)-6-amine-7-((tetrahydrofuran-3-yl)oxy)quinazolin-4-amine (**6-a**).

To a suspension of (*S*)-*N*-(3-chloro-4-fluorophenyl)-6-nitro-7-((tetrahydrofuran-3-yl)oxy)quinazolin-4-amine (2.03 g, 5 mmol) and NiCl₂·6H₂O (2.38 g, 10.0 mmol) in DCM/MeOH (32 mL: 8 mL) at 0 °C was added NaBH₄ (0.76 g, 20 mmol). After a further 30 min reaction, the reaction was evaporated in vacuo and the residue was purified by silica gel (eluent DCM/MeOH=10:1) to give light yellow solid. (yield 95%). m.p.: 162-164 °C; ¹H NMR (500 MHz, DMSO) δ 10.26 (s, 1H), 8.56 (s, 1H), 8.11 (s, 1H), 7.76 (s, 1H), 7.57 (s, 1H), 7.46 (t, *J* = 9.0 Hz, 1H), 7.24 (s, 1H), 5.70 (s, 2H), 5.22 (s, 1H), 4.02-3.99 (m, 2H), 3.95-3.91 (m, 1H), 3.81-3.80 (m, 1H), 2.36-2.32 (m, 1H), 2.15-2.13 (m, 1H); HRMS (ESI): *m/z* calcd for (C₁₈H₁₆ClFN₄O₂+H)⁺: 375.1024; found: 375.1012.

(*S*)-2-oxooxazolidine-4-carboxylic acid (**8a**).

At 0 °C, to (*L*)-carbobenzoyloxyserine (25.34 g, 106 mmol) is added a NaOH solution (8.0 g, 1.9 equiv) in 40 mL of H₂O. The solid quickly dissolves and the solution is stirred at rt for 30 min. The mixture is then washed with Et₂O (3 x 40 mL), carefully acidified to pH 1 using 37% HCl (at 0 °C), and extracted with EtOAc (12 x 50 mL). The organic layers are collected, dried over Na₂SO₄, filtered and concentrated under reduced pressure. Compound **8a** (10.21 g, 73%) is obtained as a white waxy solid. mp = 119-120 °C; [α]_D²⁰ -21 (c 0.1, H₂O); ¹H NMR (500 MHz, DMSO): δ 13.2 (brs, 1H), 8.15 (brs, 1H), 4.48 (d, *J* = 8.8 Hz, 1H), 4.38-4.26 (m, 2H).

5.2.2 General procedure for the synthesis of target compounds:

The corresponding carboxylic acid (4.0 mmol, 4.0 eq.) was dissolved in DCM, followed by adding 3 drops DMF. The suspension was cooled to 0 °C and oxalyl chloride (3.47 mmol, 3.47 eq.) was added dropwise. The mixture was stirred at 0-10 °C for 20 minutes and at 22-26 °C for 2 h, then the temperature of reaction mixture is adjusted to 40-45 °C for 5 minutes. The reaction mixture was then cooled to 0 °C. A solution of the corresponding aniline (1.0 mmol) in 6 mL DCM and a suitable volume of DMF was added dropwise then added Et₃N (5.0 mmol, 5.0 eq.). The mixture was stirred at 0-10 °C for 20 minutes then at room temperature for 3-4 h. The reaction was monitored by TLC. The reaction was quenched with saturated Na₂CO₃, extracted with EtOAc (3x20 mL) and dried over anhydrous sodium sulfate and evaporated to dryness under reduce pressure. The residue was purified through silica gel to give pure product.

(*S*)-*N*-(4-((3-chloro-4-fluorophenyl)amino)-7-methoxyquinazolin-6-yl)-2-oxooxazolidine-4-carboxamide (**9a**).

Yellow solid, yield: 90%. m.p. >250 °C; ¹H NMR (500 MHz, DMSO) δ 9.88 (s, 1H), 9.84 (s, 1H), 8.91 (s, 1H), 8.54 (s, 1H), 8.15 (s, 1H), 8.11 (d, *J* = 6.5 Hz, 1H), 7.79-7.76 (m, 1H), 7.43 (t, *J* = 9.0 Hz, 1H), 7.32 (s, 1H), 4.71-4.70 (m, 1H), 4.59 (t, *J* = 8.5 Hz, 1H), 4.35-4.33 (m, 1H), 4.03 (s, 3H); ¹³C NMR (125 MHz, DMSO) δ 169.9, 159.0, 156.9, 155.0, 154.0, 152.3, 149.1, 136.7, 126.7, 123.8, 122.6 (d, *J* = 6.3 Hz), 118.7 (d, *J* = 17.5 Hz), 118.6, 116.4 (d, *J* = 21.3 Hz), 115.4, 108.9, 106.9, 67.4, 56.4, 54.3; HRMS (ESI): *m/z* calcd for (C₁₉H₁₅ClFN₅O₄+H)⁺: 432.0875; found: 432.0895.

(*S*)-*N*-(4-((3-chloro-4-((3-fluorobenzyl)oxy)phenyl)amino)-7-ethoxyquinazolin-6-yl)-2-oxooxazolidine-4-carboxamide (**9b**).

Light yellow solid, yield: 70%. m.p. >250 °C; ¹H NMR (500 MHz, DMSO) δ 9.73 (s, 1H), 9.65 (s, 1H), 8.82 (s, 1H), 8.49 (s, 1H), 8.17 (s, 1H), 7.96 (d, *J* = 2.5 Hz, 1H), 7.68 (dd, *J* = 9.0, 2.5 Hz, 1H), 7.49-7.45 (m, 1H), 7.34-7.30 (m, 2H), 7.26-7.23 (m, 2H), 7.19 (td, *J* = 9.0, 2.0 Hz, 1H), 5.26 (s, 2H), 4.68 (dd, *J* = 9.0, 4.0 Hz, 1H), 4.61 (t, *J* = 9.0 Hz, 1H), 4.36-4.34 (m, 1H), 4.30-4.27 (m, 2H), 1.46 (t, *J* = 6.5 Hz, 3H). HRMS (ESI): *m/z* calcd for (C₂₇H₂₃ClFN₅O₅+H)⁺: 552.1450; found: 552.1480.

(*S*)-*N*-(4-((3-bromophenyl)amino)-7-methoxyquinazolin-6-yl)-2-oxooxazolidine-4-carboxamide (**9c**).

Light yellow solid, yield: 85%. m.p. >250 °C; ¹H NMR (500 MHz, DMSO) δ 9.83 (s, 1H), 9.66 (s, 1H), 8.86 (s, 1H), 8.55 (s, 1H), 8.17 (s, 1H), 8.14 (s, 1H), 7.84 (d, *J* = 8.5 Hz, 1H), 7.33 (t, *J* = 8.0 Hz, 1H), 7.28-7.26 (m, 2H), 4.69-4.66 (m, 1H), 4.61 (t, *J* = 9.0 Hz, 1H), 4.36-4.33 (m, 1H), 4.31 (q, *J* = 6.5 Hz, 2H), 1.46 (t, *J* = 6.5 Hz, 3H); HRMS (ESI): *m/z* calcd for (C₂₀H₁₈BrN₅O₄+H)⁺: 472.0620; found: 474.0593.

(*S*)-*N*-(7-methoxy-4-((3-(trifluoromethyl)phenyl)amino)quinazolin-6-yl)-2-oxooxazolidine-4-carboxamide (**9d**).

Light yellow solid, yield: 84%. m.p. >250 °C; ¹H NMR (500 MHz, DMSO) δ 10.00 (s, 1H), 9.85 (s, 1H), 8.95 (s, 1H), 8.57 (s, 1H), 8.24 (s, 1H), 8.18 (d, *J* = 8.0 Hz, 1H), 8.14 (s, 1H), 7.61 (t, *J* = 8.0 Hz, 1H), 7.43 (d, *J* = 7.5 Hz, 1H), 7.40-7.39 (m, 1H), 7.33-7.32 (m, 1H), 4.71 (dd, *J* = 9.0, 4.0 Hz, 1H), 4.58 (t, *J* = 9.5 Hz, 1H), 4.34 (dd, *J* = 9.0, 4.0 Hz, 1H), 4.04 (s, 3H); HRMS (ESI): *m/z* calcd for (C₂₀H₁₆F₃N₅O₄+H)⁺: 448.1232; found: 448.1245.

(*S*)-*N*-(4-((3-chloro-4-(pyridin-2-ylmethoxy)phenyl)amino)-7-ethoxyquinazolin-6-yl)-2-oxooxazolidine-4-carboxamide (**9e**).

Light yellow solid, yield: 70%. m.p. >250 °C; ¹H NMR (500 MHz, DMSO) δ 9.72 (s, 1H), 9.64 (s, 1H), 8.81 (s, 1H), 8.60 (d, *J* = 4.5 Hz, 1H), 8.48 (s, 1H), 8.16 (s, 1H), 7.96 (d, *J* = 2.5 Hz, 1H), 7.88 (t, *J* = 8.0 Hz, 1H), 7.67 (dd, *J* = 9.0, 2.5 Hz, 1H), 7.59 (d, *J* = 7.5 Hz, 1H), 7.38-7.36 (m, 2H), 7.26-7.24 (m, 2H), 5.29 (s, 2H), 4.68-4.66 (m, 1H), 4.61 (t, *J* = 8.5 Hz, 1H), 4.34 (dd, *J* = 9.0, 4.0 Hz, 1H), 4.29 (q, *J* = 4.5 Hz, 2H), 1.45 (t, *J* = 7.0 Hz, 3H); HRMS (ESI): *m/z* calcd for (C₂₆H₂₃ClN₆O₅+H)⁺: 535.1496; found: 535.1489.

(*S*)-*N*-(7-ethoxy-4-(((*S*)-1-phenylethyl)amino)quinazolin-6-yl)-2-oxooxazolidine-4-carboxamide (**9f**).

Light yellow solid, yield: 74%. m.p. >250 °C; ¹H NMR (500 MHz, DMSO) δ 9.59 (s, 1H), 8.69 (s, 1H), 8.42 (d, *J* = 8.0 Hz, 1H), 8.32 (s, 1H), 8.14 (s, 1H), 7.44-7.39 (m, 2H), 7.30 (t, *J* = 8.0 Hz, 2H), 7.20 (t, *J* = 7.5 Hz, 1H), 7.16 (d, *J* = 16.4 Hz, 1H), 5.61-5.58 (m, 1H), 4.64-4.58 (m, 2H), 4.35-4.33 (m, 1H), 4.26 (q, *J* = 7.0 Hz, 2H), 1.58 (d, *J* = 7.0 Hz, 3H), 1.42 (t, *J* = 7.0 Hz, 3H); HRMS (ESI): *m/z* calcd for (C₂₂H₂₃N₅O₄+H)⁺: 422.1828; found: 422.1816.

(*S*)-*N*-(7-ethoxy-4-((1-(3-fluorobenzyl)-1*H*-indazol-5-yl)amino)quinazolin-6-yl)-2-oxooxazolidine-4-carboxamide (**9g**).

Light yellow solid, yield: 70%. m.p. >250 °C; ¹H NMR (500 MHz, DMSO) δ 9.84 (s, 1H), 9.69 (s, 1H), 8.85 (s, 1H), 8.43 (s, 1H), 8.20 (s, 1H), 8.13 (d, *J* = 11.0 Hz, 2H), 7.72 (d, *J* = 9.0 Hz, 1H), 7.66 (dd, *J* = 9.0, 1.5 Hz, 1H), 7.39-7.35 (m, 1H), 7.26 (s, 1H), 7.13-7.09 (m, 1H), 7.06 (d, *J* = 7.5 Hz, 2H), 5.70 (s, 2H), 4.68 (dd, *J* = 9.0, 3.5 Hz, 1H), 4.62 (t, *J* = 9.0 Hz, 1H), 4.35 (dd, *J* = 8.5, 3.5 Hz, 1H), 4.29 (q, *J* = 7.0 Hz, 2H), 1.45 (t, *J* = 7.0 Hz, 3H); HRMS (ESI): *m/z* calcd for (C₂₈H₂₄FN₇O₄+H)⁺: 542.1952; found: 542.1939.

(*S*)-*N*-(4-((3-chloro-4-((6-methylpyridin-3-yl)oxy)phenyl)amino)-7-ethoxyquinazolin-6-yl)-2-oxooxazolidine-4-carboxamide (**9h**).

Light yellow solid, yield: 70%. m.p. >250 °C; ¹H NMR (500 MHz, DMSO) δ 9.88 (s, 1H), 9.67 (s, 1H), 8.86 (s, 1H), 8.55 (s, 1H), 8.22 (t, *J* = 2.0 Hz, 1H), 8.18-8.17 (m, 2H), 7.95 (s, 1H), 7.82 (dd, *J* = 9.0, 3.0 Hz, 1H), 7.30 (s, 1H), 7.27-7.26 (m, 2H), 7.20 (d, *J* = 9.0 Hz, 1H), 4.68 (dd, *J* = 9.0, 4.0 Hz, 1H), 4.61 (t, *J* = 8.5 Hz, 1H), 4.36-4.33 (m, 1H), 4.30 (q, *J* = 7.0 Hz, 2H), 2.45 (s, 3H), 1.47 (t, *J* = 7.0 Hz, 3H); HRMS (ESI): *m/z* calcd for (C₂₆H₂₃ClN₆O₅+H)⁺: 535.1496; found: 542.1938.

(*S*)-*N*-(4-((3-chloro-4-(cyclopropylmethoxy)phenyl)amino)-7-ethoxyquinazolin-6-yl)-2-oxooxazolidine-4-carboxamide (**9i**).

Light yellow solid, yield: 70%. m.p. >250 °C; ¹H NMR (500 MHz, DMSO) δ 9.70 (s, 1H), 9.65 (s, 1H), 8.81 (s, 1H), 8.48 (s, 1H), 8.17 (s, 1H), 7.91 (d, *J* = 2.0 Hz, 1H), 7.65 (dd, *J* = 8.5, 2.0 Hz, 1H), 7.26 (s, 1H), 7.14 (d, *J* = 9.0 Hz, 1H), 4.68-4.66 (m, 1H), 4.62-4.59 (m, 1H), 4.35-4.34 (m, 1H), 4.29 (q, *J* = 7.0 Hz, 2H), 3.92 (d, *J* = 7.0 Hz, 2H), 1.45 (t, *J* = 7.0 Hz, 3H), 0.60-0.59 (m, 2H), 0.36-0.35 (m, 2H); HRMS (ESI): *m/z* calcd for (C₂₄H₂₄ClN₅O₅+H)⁺: 498.1544; found: 498.1549.

(*S*)-*N*-(7-methoxy-4-((4-methoxyphenyl)amino)quinazolin-6-yl)-2-oxooxazolidine-4-carboxamide (**9j**).

Light yellow solid, yield: 87%. m.p. >250 °C; ¹H NMR (500 MHz, DMSO) δ 9.81 (s, 1H), 9.67 (s, 1H), 8.85 (s, 1H), 8.42 (s, 1H), 8.14 (s, 1H), 7.61 (d, *J* = 8.5 Hz, 2H), 7.26 (s, 1H), 6.98-6.93 (m, 2H), 4.69 (dd, *J* = 9.5, 4.0 Hz, 1H), 4.58 (t, *J* = 9.0 Hz, 1H), 4.33 (dd, *J* = 9.5, 4.0 Hz, 1H), 4.01 (s, 3H), 3.77 (s, 3H); HRMS (ESI): *m/z* calcd for (C₂₀H₁₉N₅O₅+H)⁺: 410.1464; found: 410.1435.

(*S*)-*N*-(4-((3-chloro-4-fluorophenyl)amino)-7-(((*S*)-tetrahydrofuran-3-yl)oxy)quinazolin-6-yl)-2-oxooxazolidine-4-carboxamide (**9k**).

Light yellow solid, yield: 75%. m.p.: 223-225 °C; ¹H NMR (500 MHz, DMSO) δ 9.88 (s, 1H), 9.59 (s, 1H), 8.84 (s, 1H), 8.54 (s, 1H), 8.19 (s, 1H), 8.12 (dd, *J* = 7.0, 2.5 Hz, 1H), 7.80-7.77 (m, 1H), 7.43 (t, *J* = 9.0 Hz, 1H), 7.27 (s, 1H), 5.32-5.30 (m, 1H), 4.67 (dd, *J* = 9.0, 3.5 Hz, 1H), 4.61 (t, *J* = 9.0 Hz, 1H), 4.35 (dd, *J* = 9.0, 3.5 Hz, 1H), 4.03-4.00 (m, 1H), 3.97-3.91 (m, 2H), 3.82-3.78 (m, 1H), 2.37-2.33 (m, 1H), 2.13-2.10 (m, 1H); HRMS (ESI): *m/z* calcd for (C₂₂H₁₉ClFN₅O₅+H)⁺: 488.1137; found: 488.1124.

(*S*)-*N*-(4-((3-chloro-4-fluorophenyl)amino)-7-(((*S*)-1-methylpyrrolidin-3-yl)oxy)quinazolin-6-yl)-2-oxooxazolidine-4-carboxamide (**9l**).

Yellow solid, yield: 70%. m.p.: 213-215 °C; ¹H NMR (500 MHz, DMSO) δ 9.88 (s, 1H), 9.66 (s, 1H), 8.84 (s, 1H), 8.53 (s,

1H), 8.21-8.19 (m, 1H), 8.12 (dd, *J* = 6.5, 2.5 Hz, 1H), 7.80-7.77 (m, 1H), 7.43 (t, *J* = 9.0 Hz, 1H), 7.20 (s, 1H), 5.14 (m, 1H), 4.68 (m, 1H), 4.62 (t, *J* = 9.0 Hz, 1H), 4.36 (dd, *J* = 8.5, 3.5 Hz, 1H), 2.84-2.82 (m, 2H), 2.41 (m, 2H), 2.31 (s, 3H), 2.04-1.95 (m, 1H); HRMS (ESI): *m/z* calcd for (C₂₃H₂₂ClFN₆O₄+H)⁺: 501.1453; found: 501.1437.

(*S*)-*N*-(4-((3-chloro-2,4-difluorophenyl)amino)-7-((1-methylpiperidin-4-yl)methoxy)quinazolin-6-yl)-2-oxooxazolidine-4-carboxamide (**9m**).

Yellow solid, yield: 70%. m.p.: 204-205 °C; ¹H NMR (500 MHz, DMSO) δ 9.93 (s, 1H), 9.61 (s, 1H), 8.79 (s, 1H), 8.41 (s, 1H), 7.54-7.49 (m, 1H), 7.38 (t, *J* = 8.0 Hz, 1H), 7.32-7.30 (m, 1H), 4.689-4.67 (m, 1H), 4.62 (t, *J* = 9.0 Hz, 1H), 4.49-4.42 (m, 1H), 4.33 (dd, *J* = 8.5, 4.0 Hz, 1H), 4.10 (t, *J* = 6.5 Hz, 1H), 3.10 (m, 2H), 2.46 (s, 3H), 1.98-1.91 (m, 4H), 1.54-1.50 (m, 2H); HRMS (ESI): *m/z* calcd for (C₂₅H₂₅ClF₂N₆O₄+H)⁺: 547.1672; found: 547.1710.

(*S*)-*N*-(4-((3-chloro-4-fluorophenyl)amino)-7-(2,2,2-trifluoroethoxy)quinazolin-6-yl)-2-oxooxazolidine-4-carboxamide (**9n**).

Light yellow solid, yield: 75%. m.p. > 250 °C; ¹H NMR (500 MHz, DMSO) δ 9.94 (s, 1H), 9.84 (s, 1H), 8.73 (s, 1H), 8.59 (s, 1H), 8.17 (s, 1H), 8.14 (dd, *J* = 7.0, 2.5 Hz, 1H), 7.95 (s, 1H), 7.81-7.78 (m, 1H), 7.51 (s, 1H), 7.45 (t, *J* = 9.0 Hz, 1H), 5.06 (q, *J* = 8.5 Hz, 2H), 4.63-4.62 (m, 2H), 4.31-4.30 (m, 1H); HRMS (ESI): *m/z* calcd for (C₂₀H₁₄ClF₄N₅O₄+H)⁺: 500.0748; found: 500.0729.

(*S*)-*N*-(4-((3-chloro-4-fluorophenyl)amino)-7-(((*R*)-4-methylmorpholin-3-yl)methoxy)quinazolin-6-yl)-2-oxooxazolidine-4-carboxamide (**9o**).

Light yellow solid, yield: 55%. m.p. > 250 °C; ¹H NMR (500 MHz, DMSO) δ 9.89 (s, 1H), 9.67 (s, 1H), 8.76 (s, 1H), 8.56 (s, 1H), 8.22 (s, 1H), 8.14 (dd, *J* = 5.0, 2.5 Hz, 1H), 7.81-7.78 (m, 1H), 7.44 (t, *J* = 9.0 Hz, 1H), 7.37 (s, 1H), 4.64-4.610 (m, 2H), 4.40-4.35 (m, 2H), 4.16-4.13 (m, 1H), 3.96-3.94 (m, 1H), 3.74-3.72 (m, 1H), 3.57 ((t, *J* = 10.0 Hz, 1H), 3.44 (t, *J* = 10.0 Hz, 1H), 2.59 (m, 1H), 2.33 (s, 3H), 2.28 (m, 1H); HRMS (ESI): *m/z* calcd for (C₂₄H₂₄ClFN₆O₅+H)⁺: 531.1559; found: 531.1552.

(*S*)-*N*-(4-((3-chloro-4-fluorophenyl)amino)-7-(2-methoxyethoxy)quinazolin-6-yl)-2-oxooxazolidine-4-carboxamide (**9p**).

Light yellow solid, yield: 89%. m.p. > 250 °C; ¹H NMR (500 MHz, DMSO) δ 9.89 (s, 1H), 9.71 (s, 1H), 8.81 (s, 1H), 8.54 (s, 1H), 8.18 (s, 1H), 8.13 (dd, *J* = 7.0, 3.0 Hz, 1H), 7.81-7.80 (m, 1H), 7.43 (t, *J* = 9.0 Hz, 1H), 7.34 (s, 1H), 4.65-4.62 (m, 2H), 4.37-4.36 (m, 3H), 3.79-3.78 (m, 2H), 3.35 (s, 3H); HRMS (ESI): *m/z* calcd for (C₂₁H₁₉ClFN₅O₅+H)⁺: 476.1137; found: 476.1174.

(*S*)-*N*-(4-((3-chloro-4-fluorophenyl)amino)-7-(2-(piperidin-1-yl)ethoxy)quinazolin-6-yl)-2-oxooxazolidine-4-carboxamide (**9q**).

Yellow solid, yield: 89%. m.p.: 203-205 °C; ¹H NMR (500 MHz, DMSO) δ 9.86 (s, 1H), 9.64 (s, 1H), 8.81 (s, 1H), 8.54 (s, 1H), 8.18 (s, 1H), 8.12 (dd, *J* = 6.5, 2.5 Hz, 1H), 7.80-7.77 (m, 1H), 7.42 (t, *J* = 9.0 Hz, 1H), 7.34 (s, 1H), 4.63-4.60 (m, 2H), 4.37-4.36 (m, 1H), 4.33 (t, *J* = 6.0 Hz, 2H), 2.79 (m, 2H), 1.52-1.50 (m, 5H), 1.40-1.39 (m, 3H), 1.18 (t, *J* = 7.0 Hz, 1H); HRMS (ESI): *m/z* calcd for (C₂₅H₂₆ClFN₅O₄+H)⁺: 529.1766; found: 529.1760.

(*S*)-*N*-(4-((3-chloro-4-fluorophenyl)amino)-7-(3-morpholinopropoxy)quinazolin-6-yl)-2-oxooxazolidine-4-carboxamide (**9r**).

Light yellow solid, yield: 75%. m.p.:234-236 °C; ¹H NMR (500 MHz, DMSO) δ 9.86 (s, 1H), 9.63 (s, 1H), 8.81 (s, 1H), 8.54 (s, 1H), 8.19 (s, 1H), 8.12 (dd, *J* = 7.0, 2.5 Hz, 1H), 7.80-7.77 (m, 1H), 7.43 (t, *J* = 9.0 Hz, 1H), 7.31 (s, 1H), 4.65-4.62 (m, 2H), 4.34 (dd, *J* = 8.0, 3.5 Hz, 1H), 4.28 (t, *J* = 6.0 Hz, 2H), 3.59 (t, *J* = 4.5 Hz, 4H), 2.40 (m, 3H), 2.01-1.98 (m, 2H); HRMS (ESI): *m/z* calcd for (C₂₅H₂₆ClFN₆O₅+H)⁺: 545.1715; found: 545.1712.

(*R*)-*N*-(4-((3-chloro-4-fluorophenyl) amino)-7-methoxyquinazolin-6-yl)-2-oxooxazolidine-4-carboxamide (**10a**).

Light yellow solid, yield: 85%. m.p. >250 °C; ¹H NMR (500 MHz, DMSO) δ 9.88 (s, 1H), 9.84 (s, 1H), 8.90 (s, 1H), 8.54 (s, 1H), 8.14 (s, 1H), 8.11 (dd, *J* = 7.0, 2.5 Hz, 1H), 7.80-7.76 (m, 1H), 7.43 (t, *J* = 9.0 Hz, 1H), 7.32 (s, 1H), 4.70 (dd, *J* = 9.5, 4.0 Hz, 1H), 4.58 (t, *J* = 9.0 Hz, 1H), 4.33 (dd, *J* = 9.5, 4.0 Hz, 1H), 4.03 (s, 3H); HRMS (ESI): *m/z* calcd for (C₁₉H₁₅ClFN₅O₄+H)⁺: 432.0875; found: 432.0868.

(*R*)-*N*-(4-((3-chloro-4-((3-fluorobenzyl) oxy) phenyl) amino)-7-ethoxyquinazolin-6-yl)-2-oxooxazolidine-4-carboxamide (**10b**).

Light yellow solid, yield: 70%. m.p. >250 °C; ¹H NMR (500 MHz, DMSO) δ 9.72 (s, 1H), 9.64 (s, 1H), 8.81 (s, 1H), 8.48 (s, 1H), 8.16 (s, 1H), 7.95 (d, *J* = 2.5 Hz, 1H), 7.67 (dd, *J* = 9.0, 2.5 Hz, 1H), 7.50-7.45 (m, 1H), 7.34-7.30 (m, 2H), 7.26-7.23 (m, 2H), 7.18-7.16 (m, 1H), 5.25 (s, 2H), 4.67 (dd, *J* = 9.0, 4.0 Hz, 1H), 4.61 (t, *J* = 9.0 Hz, 1H), 4.34 (dd, *J* = 8.5, 4.0 Hz, 1H), 4.29 (q, *J* = 7.0 Hz, 2H), 1.45 (dd, *J* = 7.0 Hz, 3H). HRMS (ESI): *m/z* calcd for (C₂₇H₂₃ClFN₅O₅+K)⁺: 590.1009; found: 590.1015.

(*R*)-*N*-(4-((3-bromophenyl) amino)-7-methoxyquinazolin-6-yl)-2-oxooxazolidine-4-carboxamide (**10c**).

Yellow solid, yield: 80%. m.p. >250 °C; ¹H NMR (500 MHz, DMSO) δ 9.86-9.85 (m, 2H), 8.92 (s, 1H), 8.56 (s, 1H), 8.14 (d, *J* = 5.0 Hz, 2H), 7.84 (d, *J* = 8.0 Hz, 1H), 7.40-7.39 (m, 1H), 7.33-7.31 (m, 2H), 5.19-5.16 (m, 1H), 4.60-4.57 (m, 1H), 4.54-4.48 (m, 1H), 4.03 (s, 3H); HRMS (ESI): *m/z* calcd for (C₁₉H₁₆BrN₅O₄+H)⁺: 458.0464; found: 460.0144.

(*R*)-*N*-(4-((3-chloro-4-(pyridin-2-ylmethoxy) phenyl) amino)-7-ethoxyquinazolin-6-yl)-2-oxooxazolidine-4-carboxamide (**10e**).

Light yellow solid, yield: 80%. m.p. >250 °C; ¹H NMR (500 MHz, DMSO) δ 9.72 (s, 1H), 9.64 (s, 1H), 8.81 (s, 1H), 8.60 (d, *J* = 4.5 Hz, 1H), 8.48 (s, 1H), 8.16 (s, 1H), 7.96 (d, *J* = 2.5 Hz, 1H), 7.90-7.87 (m, 1H), 7.67 (dd, *J* = 9.0, 3.0 Hz, 1H), 7.59 (d, *J* = 7.5 Hz, 1H), 7.38-7.36 (m, 1H), 7.26-7.24 (m, 2H), 5.29 (s, 2H), 4.68-4.66 (m, 1H), 4.60 (t, *J* = 8.5 Hz, 1H), 4.34 (dd, *J* = 9.0, 4.0 Hz, 1H), 4.29 (q, *J* = 7.0 Hz, 2H), 1.46 (d, *J* = 7.0 Hz, 3H); HRMS (ESI): *m/z* calcd for (C₂₆H₂₃ClN₆O₅+H)⁺: 535.1496; found: 535.1487.

(*R*)-*N*-(7-ethoxy-4-(((*S*)-1-phenylethyl) amino) quinazolin-6-yl)-2-oxooxazolidine-4-carboxamide (**10f**).

Yellow solid, yield: 74%. m.p. >250 °C; ¹H NMR (500 MHz, DMSO) δ 9.72 (s, 1H), 9.03 (s, 1H), 8.79 (s, 1H), 8.49 (s, 1H), 8.16-8.14 (m, 2H), 7.45 (d, *J* = 7.5 Hz, 2H), 7.33 (t, *J* = 7.5 Hz, 3H), 7.25-7.22 (m, 2H), 5.70-5.67 (m, 1H), 4.67-4.66 (m, 1H), 4.60 (t, *J* = 8.5 Hz, 1H), 4.50-4.47 (m, 1H), 4.36-4.34 (m, 2H), 4.31-4.24 (m, 3H), 1.60 (d, *J* = 7.0 Hz, 3H), 1.44 (t, *J* = 6.5 Hz,

3H); HRMS (ESI): *m/z* calcd for (C₂₂H₂₃N₅O₄+H)⁺: 422.1828; found: 422.1366.

(*R*)-*N*-(7-ethoxy-4-((1-(3-fluorobenzyl)-1*H*-indazol-5-yl) amino) quinazolin-6-yl)-2-oxooxazolidine-4-carboxamide (**10g**).

Yellow solid, yield: 70%. m.p. >250 °C; ¹H NMR (500 MHz, DMSO) δ 9.84 (s, 1H), 9.69 (s, 1H), 8.85 (s, 1H), 8.43 (s, 1H), 8.20 (s, 1H), 8.14 (s, 1H), 8.12 (s, 1H), 7.72 (d, *J* = 9.0 Hz, 1H), 7.68-7.63 (m, 1H), 7.43-7.35 (m, 2H), 7.25 (s, 1H), 7.11 (t, *J* = 8.0 Hz, 1H), 7.06 (d, *J* = 8.0 Hz, 2H), 5.70 (s, 2H), 4.67 (dd, *J* = 9.0, 3.5 Hz, 1H), 4.61 (t, *J* = 8.5 Hz, 1H), 4.34 (dd, *J* = 9.0, 4.0 Hz, 1H), 4.29 (q, *J* = 7.0 Hz, 2H), 1.45 (t, *J* = 7.0 Hz, 3H); HRMS (ESI): *m/z* calcd for (C₂₈H₂₄FN₇O₄+H)⁺: 542.1952; found: 542.1939.

(*R*)-*N*-(4-((3-chloro-4-fluorophenyl)amino)-7-(((*S*)-tetrahydrofuran-3-yl)oxy) quinazolin-6-yl)-2-oxooxazolidine-4-carboxamide (**10h**).

Light yellow solid, yield: 78%. m.p.:223-225 °C; ¹H NMR (500 MHz, DMSO) δ 9.87 (s, 1H), 9.59 (s, 1H), 8.83 (s, 1H), 8.54 (s, 1H), 8.19 (s, 1H), 8.12 (dd, *J* = 6.5, 2.5 Hz, 1H), 7.80-7.77 (m, 1H), 7.43 (t, *J* = 9.0 Hz, 1H), 7.27 (s, 1H), 5.32-5.30 (m, 1H), 4.67 (dd, *J* = 9.0, 3.0 Hz, 1H), 4.61 (t, *J* = 8.5 Hz, 1H), 4.35 (dd, *J* = 8.5, 3.5 Hz, 1H), 4.03-4.00 (m, 1H), 3.96-3.90 (m, 2H), 3.82-3.78 (m, 1H), 2.38-2.31 (m, 1H), 2.16-2.11 (m, 1H); HRMS (ESI): *m/z* calcd for (C₂₂H₁₉ClFN₅O₅+H)⁺: 488.1137; found: 488.1139.

(*R*)-*N*-(4-((3-chloro-2, 4-difluorophenyl) amino)-7-((1-methylpiperidin-4-yl) methoxy) quinazolin-6-yl)-2-oxooxazolidine-4-carboxamide (**10i**).

Light yellow solid, yield: 65%. m.p.:206-207 °C; ¹H NMR (500 MHz, DMSO) δ 9.93 (s, 1H), 9.61 (s, 1H), 8.79 (s, 1H), 8.41 (s, 1H), 7.54-7.49 (m, 1H), 7.38 (t, *J* = 8.0 Hz, 1H), 7.32-7.30 (m, 1H), 4.66-4.60 (m, 3H), 4.33 (dd, *J* = 8.5, 3.0 Hz, 1H), 4.10 (t, *J* = 6.5 Hz, 1H), 2.89-2.80 (m, 2H), 2.24 (s, 3H), 1.90-1.84 (m, 4H), 1.41-1.37 (m, 2H); HRMS (ESI): *m/z* calcd for (C₂₅H₂₅ClF₂N₆O₄+H)⁺: 547.1672; found: 547.1661.

(*R*)-*N*-(4-((3-chloro-4-fluorophenyl)amino)-7-(2-methoxyethoxy)quinazolin-6-yl)-2-oxooxazolidine-4-carboxamide (**10j**).

Light yellow solid, yield: 89%. m.p. > 250 °C; ¹H NMR (500 MHz, DMSO) δ 9.93 (s, 1H), 9.79 (s, 1H), 8.81 (s, 1H), 8.54 (s, 1H), 8.14 (d, *J* = 6.0 Hz, 1H), 7.80 (m, 1H), 7.43 (t, *J* = 9.0 Hz, 1H), 7.33 (s, 1H), 4.66 (m, 1H), 4.63-4.60 (m, 1H), 4.40-4.33 (m, 3H), 3.79-3.76 (m, 2H), 3.35 (s, 3H); HRMS (ESI): *m/z* calcd for (C₂₁H₁₉ClFN₅O₅+H)⁺: 476.1137; found: 476.1155.

(*R*)-*N*-(4-((3-chloro-4-fluorophenyl)amino)-7-(3-morpholinopropoxy)quinazolin-6-yl)-2-oxooxazolidine-4-carboxamide (**10l**).

Light yellow solid, yield: 65%. m.p.:228-229 °C; ¹H NMR (500 MHz, DMSO) δ 9.87 (s, 1H), 9.64 (s, 1H), 8.82 (s, 1H), 8.54 (s, 1H), 8.20 (s, 1H), 8.12 (d, *J* = 5.0 Hz, 1H), 7.80-7.77 (m, 1H), 7.43 (t, *J* = 9.5 Hz, 1H), 7.31 (s, 1H), 4.65-4.62 (m, 2H), 4.34 (dd, *J* = 8.0, 3.0 Hz, 1H), 4.27 (t, *J* = 6.0 Hz, 2H), 3.59 (m, 4H), 2.40 (m, 4H), 2.02-1.99 (m, 2H); HRMS (ESI): *m/z* calcd for (C₂₅H₂₆ClFN₆O₅+H)⁺: 545.1715; found: 545.1729.

(4*S*,5*R*)-*N*-(4-((3-chloro-4-fluorophenyl)amino)-7-methoxyquinazolin-6-yl)-5-methyl-2-oxooxazolidine-4-carboxamide (**11a**).

Light yellow solid, yield: 70%. m.p. >250 °C; ¹H NMR (500 MHz, DMSO) δ 9.88 (s, 1H), 9.84 (s, 1H), 8.87 (s, 1H), 8.55 (s, 1H), 8.11 (t, *J* = 5.0 Hz, 2H), 7.80-7.77 (m, 1H), 7.43 (t, *J* = 9.0 Hz, 1H), 7.32 (s, 1H), 4.64-4.62 (m, 1H), 4.33 (d, *J* = 4.5 Hz, 1H), 4.04 (s, 3H), 1.47 (d, *J* = 6.5 Hz, 3H); HRMS (ESI): *m/z* calcd for (C₂₀H₁₇ClFN₅O₄+H)⁺: 446.1031; found: 446.1030.

(4*S*,5*R*)-*N*-(4-((3-chloro-4-((3-fluorobenzyl)oxy)phenyl)amino)-7-ethoxyquinazolin-6-yl)-5-methyl-2-oxooxazolidine-4-carboxamide (**11b**).

Light yellow solid, yield: 70%. m.p. >250 °C; ¹H NMR (500 MHz, DMSO) δ 9.84 (s, 1H), 9.77 (s, 1H), 8.84 (s, 1H), 8.50 (s, 1H), 8.12 (s, 1H), 7.95 (d, *J* = 3.5 Hz, 2H), 7.67 (d, *J* = 8.5 Hz, 1H), 7.48 (dd, *J* = 14.0, 8.0 Hz, 1H), 7.37-7.30 (m, 3H), 7.25 (d, *J* = 9.0 Hz, 1H), 7.19 (t, *J* = 10.0 Hz, 1H), 5.25 (s, 2H), 4.63 (t, *J* = 5.5 Hz, 1H), 4.32 (d, *J* = 3.5 Hz, 1H), 4.03 (s, 3H), 1.46 (d, *J* = 6.5 Hz, 3H); HRMS (ESI): *m/z* calcd for (C₂₇H₂₃ClFN₅O₅+H)⁺: 552.1450; found: 552.1435.

(4*S*,5*R*)-*N*-(4-((3-chloro-4-(cyclopropylmethoxy)phenyl)amino)-7-ethoxyquinazolin-6-yl)-5-methyl-2-oxooxazolidine-4-carboxamide (**11c**).

Light yellow solid, yield: 70%. m.p. >250 °C; ¹H NMR (500 MHz, DMSO) δ 9.71 (s, 1H), 9.66 (s, 1H), 8.76 (s, 1H), 8.48 (s, 1H), 8.15 (s, 1H), 7.91 (d, *J* = 2.5 Hz, 1H), 7.65 (dd, *J* = 9.0, 2.5 Hz, 1H), 7.26 (s, 1H), 7.13 (d, *J* = 9.0 Hz, 1H), 4.64-4.62 (m, 1H), 4.30-4.26 (m, 2H), 3.92 (d, *J* = 7.0 Hz, 2H), 1.50-1.43 (m, 6H), 1.28-1.21 (m, 1H), 0.62-0.57 (m, 2H), 0.38-0.34 (m, 2H); HRMS (ESI): *m/z* calcd for (C₂₅H₂₆ClN₅O₅+H)⁺: 512.9652; found: 512.9635.

(*S*)-*N*-(4-((3-chloro-4-fluorophenyl)amino)-7-methoxyquinazolin-6-yl)-5-oxopyrrolidine-2-carboxamide (**12a**).

Yellow solid, yield: 85%. m.p. > 250 °C; ¹H NMR (500 MHz, DMSO) δ 9.85 (s, 1H), 9.61 (s, 1H), 8.88 (s, 1H), 8.53 (s, 1H), 8.10 (dd, *J* = 7.0, 2.5 Hz, 1H), 8.01 (s, 1H), 7.80-7.77 (m, 1H), 7.42 (t, *J* = 9.0 Hz, 1H), 7.31 (s, 1H), 4.45 (dd, *J* = 8.5, 3.5 Hz, 1H), 4.03 (s, 3H), 2.45-2.37 (m, 1H), 2.30-2.23 (m, 1H), 2.20-2.13 (m, 1H), 2.09-2.03 (m, 1H); HRMS (ESI): *m/z* calcd for (C₂₀H₁₇ClFN₃O₃+H)⁺: 430.1082; found: 430.1035.

5.3 Biological evaluation

5.3.1 Cell growth assay

The human epidermal carcinoma cell A431^{EGFR^{WT}}, NSCLC cancer cell NCI-H1975^{EGFR^{L858R/T790M}}, human lung cancer cell A549^{EGFR^{WT/K-Ras}} and human hepatic cancer cell HepG2 were used to evaluate the potency and toxicity of synthesized analogues in cell-based level. All the cell lines were purchased from American type culture collection (ATCC). A431, A549 and HepG2 were cultured with RPMI 1640 (GIBCO), NCI-H1975 was cultured with Dulbecco's Modified Eagle's Medium (GIBCO). All the mediums were supplemented with penicillin, streptomycin and 10% fetal bovine serum. The cancer cells were seeded in density of 3500 cells/well, in 96-well plates (Corning) for 24 hours. Duplicate wells were treated with test or reference compounds for 72 hours at various concentrations or DMSO (Sigma) as control. Plates were incubated at 37 °C in 5% CO₂ atmosphere. The IC₅₀ was calculated using GraphPad Prism 5.0.

5.3.2 Kinase inhibitory assay

The assays were performed *in vitro* using Homogeneous time-resolved fluorescence (HTRF) method (Cisbio). EGFR^{L858R}, EGFR^{T790M} and EGFR^{WT} were purchased from Sigma. The kinases

and substrates were incubated first with synthesized analogues for 5 minutes in enzymatic buffer. Then ATP (Sigma) was added into the reaction mixture to start the enzyme reaction. The ATP concentrations used in each enzyme reaction were 1.65 μM for EGFR, equivalent to the K_m of ATP for the corresponding enzyme in this assay condition. The assays were conducted at room temperature for 30 minutes and stopped by detection reagents which contain EDTA. The detection step lasted for 1 hour. The IC₅₀ was calculated using GraphPad Prism 5.0.

5.3.3 Western blotting assay

A431 cells (5 x 10⁵ /well) were seeded in 6-well plates overnight. Cell were exposed to 1 μM synthesized analogues for 1 h at 37 °C and then either immediately treated with media containing EGF (20 ng/ml) for 15 min or thoroughly washed with fresh medium 10 times for 5 h before EGF treatment. Whole cell lysates were prepared and total protein concentrations were determined. Proteins were extracted with lysis buffer (50 mM Tris-HCl, 150 mM NaCl, 1 mM EDTA, 0.1% SDS, 0.5% deoxycholic acid, 0.02% sodium azide, 1% NP-40, 2.0 μg/ml aprotinin, 1 mM phenylmethylsulfonyl fluoride). The lysates were centrifuged at 13,000 rpm for 30 min at 4 °C. Equivalent amounts of proteins were loaded on SDS-PAGE gels for electrophoresis and were subjected to transfer onto PVDF membranes. Appropriate antibodies to EGFR and p-EGFR from Cell Signalling Technology (Danvers, MA) and anti-β-actin from Santa Cruz Biotech (Santa Cruz, CA) were used. Proteins were visualized with peroxidase-coupled secondary antibody from Southern Biotech (Birmingham, UK), using ECL-plus kit from Amersham Biosciences (UK) for detection.

5.3.4 Stability study

Chemical stability was tested under physiological (0.2 M PBS, pH 7.4), and alkaline (0.2 M PBS, pH 9.0 or pH 10.0) pH conditions, at 37 °C. Stock solutions of test compounds were prepared in CH₃CN, and each sample was incubated at a final concentration of 50 μM in pre-warmed buffered solutions. At regular time points, aliquots were sampled and immediately injected into the LC-TOF MS system.

5.3.5 Determination of GSH conjugation

Reactions of compound **9b** or Canertinib with GSH were monitored with Agilent 1290 HPLC-6224 Time of Flight Mass Spectrometer. Reactions were initiated by mixing 10 μL of the tested compounds (5 mM in MeCN) with 10 μL of GSH (500 mM in PBS, pH=7.4). Final solutions in 200 μL PBS (Costar flat-bottom clear 96-well plate, 300 μL per well), containing 50 μM compound **9b** or canertinib and 5 mM of GSH were incubated for 1440 min at room temp prior to acquiring absorption spectra (214 nm). Formation of the thioether was quantified by area normalization method based on the peak area on HPLC spectrum.

5.3.6 Computational methods for molecular docking

The molecular modeling simulations were performed using Tripos Sybyl x1.3 molecular modeling package.^[16] The co-crystal structure of EGFR^[T790M] in complex with afatinib was obtained from the RSC Protein Data Bank (<http://www.rcsb.org>) (PDB code: 4G5P). The missing hydrogen atoms were added to the co-crystal structure using Biopolymer module in Sybyl x1.3. The initial structure of **9a** was generated by Sketch module in Sybyl x1.3. The geometries of the compound was subsequently optimized using the Tripos force field with Gasteiger-Hückel charges. The produced conformation of **9a** was then inserted into

the binding pocket of EGFR^[T790M] to replace ligand dacomitinib for the initial structural model of **9a** binding to EGFR^[T790M]. Molecular docking studies of **9a** with the EGFR^[T790M] binding pocket was performed with FlexiDock module in Sybyl 6.9.^[17] The docked complexes of inhibitor-enzyme were selected according to the criteria of interacting energy combined with geometrical matching quality. These complexes were used as the starting conformation for the geometrical optimization to achieve the final models of **9a** binding to EGFR^[T790M].

Acknowledgments

This project was supported from the National Natural Science Foundation of China (No. 81273356 and 81473074), National Science & Technology Major Projects for "Major New Drugs Innovation and Development" of China (2014ZX09304002-007), the Program for Zhejiang Leading Team of S&T Innovation Team (2011R50014) and Arthritis & Chronic Pain Research Institute, USA to Y. Yu; National Natural Science Foundation of China (No. 81402778) and the Fundamental Research Funds for the Central Universities (No. 2015QNA7029) to W. Chen; the China Postdoctoral Science Foundation Funded Project (2015M570520) to J. Shao. We appreciate Marc A. Giulianotti (Torrey Pines Institute for Molecular Studies, USA) for critical reading of the manuscript.

References and notes

- R. Siegal, J. Ma, Z. Zou, A.J. DVM, Cancer statistics, 2014, *CA Cancer J. Clin.* **2014**, *64*, 9-29.
- A. Matikas, D. Mistriotis, V. Georgoulis, A. Kotaskis, Current and future approaches in the management of non-small-cell lung cancer patients with resistance to EGFR TKIs, *Clin. Lung Cancer* **2015**, *16*, 252-261.
- N. E. Hynes, H. A. Lane, ERBB receptors and cancer: the complexity of targeted inhibitors. *Nat. Rev. Cancer* **2005**, *97*, 339-346.
- E. Castañón, P. Martín, C. Rolfo, J. P. Fusco, L. Ceniceros, J. Legaspi, M. Santisteban, I. Gil-Bazo, Epidermal Growth Factor Receptor targeting in non-small cell lung cancer: revisiting different strategies against the same target. *Curr. Drug Targets* **2014**, *15*, 1273-1283.
- M.H. Cohen, G.A. Williams, R. Sridhara, G. Chen, W.D.Jr. McGuinn, D. Morse, S. Abraham, A. Rahman, C. Liang, R. Lostritto, A. Baird, R. Pazdur, United States Food and Drug Administration Drug Approval summary: Gefitinib (ZD1839; Iressa) tablets. *Clin. Cancer Res.* **2004**, *10*, 1212-1218.
- C. Zhou, Y.L. Wu, G. Chen, J. Feng, X.Q. Liu, C. Wang, S. Zhang, J. Wang, S. Zhou, S. Ren, S. Lu, L. Zhang, C. Hu, C. Hu, Y. Luo, L. Chen, M. Ye, J. Huang, X. Zhi, Y. Zhang, Q. Xiu, J. Ma, L. Zhang, C. You, Erlotinib versus chemotherapy as first-line treatment for patients with advanced EGFR mutation-positive non-small-cell lung cancer (OPTIMAL, CTONG-0802): a multicentre, open-label, randomised, phase 3 study. *Lancet Oncol.* **2011**, *12*, 735-742.
- H.A. Yu, M.E. Arcila, N. Rekhtman, C.S. Sima, M.F. Zakowski, W. Pao, M.G. Kris, V.A. Miller, M. Ladanyi, G.J. Riely Analysis of tumor specimens at the time of acquired resistance to EGFR-TKI therapy in 155 patients with EGFR-mutant lung cancers. *Clin. Cancer Res.* **2013**, *19*, 2240-2247.
- C. H. Yun, K. E. Mengwasser, A.V. Toms, M.S. Woo, H. Greulich, K.K. Wong, M. Meyerson, M.J. Eck, The T790M mutation in EGFR kinase causes drug resistance by increasing the affinity for ATP. *Proc. Natl. Acad. Sci. USA*, **2008**, *105*, 2240-2247.
- FDA approves afatinib for advanced lung cancer. *Oncology (Williston Park)* **2013**, *27*, 813-814.
- L. V. Sequist, J. C. Soria, J. W. Goldman, H. A. Wakelee, S. M. Gadgeel, A. Varga, V. Papadimitrakopoulou, B. J. Solomon, G. R. Oxnard, R. Dziadziuszko, D. L. Aisner, R. C. Doebele, C. Galasso, E. B. Garon, R. S. Heist, J. Logan, J. W. Neal, M. A. Mendenhall, S. Nichols, Z. Piotrowska, A. J. Wozniak, M. Raponi, C. A. Karlovich, S. Jaw-Tsai, J. Isaacson, D. Despain, S. L. Matheny, L. Rolfé, A. R. Allen, D. R. Camidge, Rocicetinib in EGFR mutated non-small-cell lung cancer. *N. Engl. J. Med.* **2015**, *372*, 1700-1709.
- D. A. E. Cross, S. E. Ashton, S. Giorghiu, C. Eberlein, C. A. Nebhan, P. J. Spitzler, J. P. Orme, M. R. V. Finlay, R. A. Ward, M. J. Mellor, G. Hughes, A. Rahi, V. N. Jacobs, M. R. Brewer, E. Ichihara, J. Sun, H. Jin, P. Ballard, K. Al-Kadhimi, R. Rowlinson, T. Klinowska, G. H. P. Richmond, M. Cantarini, D.-W. Kim, M. R. Ranson, W. Pao, AZD9291, an irreversible EGFR TKI, overcomes T790M-mediated resistance to EGFR inhibitors in lung cancer. *Cancer Discov.* **2014**, *4*, 1046-1061.
- a) K. S. Thress1, C. P. Paweletz, E. Felip, B. C. Cho, D. Stetson1, B. Dougher, Z. Lai, A. Markovets, A. Vivanco, Y. Kuang, D. Ercan, S. E. Matthews, M. Cantarini, J. C. Barrett, P.A. Jänne, G. R Oxnard, Acquired EGFR C797S mutation mediates resistance to AZD9291 in non-small cell lung cancer harboring EGFR T790M. *Nat. Med.* **2015**, *21*, 560-564.b) D. Ercan, H. G. Choi, C.-H. Yun, M. Capelletti, T. Xie, M. J. Eck, N. S. Gray, and P. A. Jänne, EGFR mutations and resistance to irreversible pyrimidine-based EGFR inhibitors. *Clin. Cancer Res.* **2015**, *21*, 3913-3923. c) M. J. Niederst, H. Hu, H. E. Mulvey, E. L. Lockerman, A. R. Garcia, Z. Piotrowska, L. V. Sequist, J. A. Engelman, *Clin. Cancer Res.* **2015**, *21*, 3924-3933.
- a)Y. Zhang, Z. Chen, Y. Lou, Y. Yu, 2,3-Disubstituted 8-aryl-amino-3H-imidazo[4,5-g]quinazolines: A novel class of antitumor agents. *Eur. J. Med. Chem.* **2009**, *44*, 448-452. b) J. Wu, W. Chen, G. Xia, J. Zhang, J. Shao, B. Tan, C. Zhang, W. Yu, Q. Weng, H. Liu, M. Hu, H. Deng, Y. Hao, J. Shen, Y. Yu, Design, synthesis, and biological evaluation of novel conformationally constrained inhibitors targeting EGFR. *ACS Med. Chem. Lett.* **2013**, *4*, 974-978. c) G. Xia, W. Chen, J. Zhang, J. Shao, Y. Zhang, W. Huang, L. Zhang, W. Qi, X. Sun, B. Li, Z. Xiang, C. Ma, J. Xu, H. Deng, Y. Li, P. Li, H. Miao, J. Han, Y. Liu, J. Shen, Y. Yu, A chemical tuned strategy to develop novel irreversible EGFR-TK inhibitors with improved safety and pharmacokinetic profiles. *J. Med. Chem.* **2014**, *57*, 9889-9900.
- L. Moisan, P. Thuéry, M. Nicolas, E. Doris, B. Rousseau, Formal synthesis of (+)-catharanthine. *Angew. Chem. Int. Ed.* **2006**, *45*, 5334-5336.
- H. Ishibashi, M. Uegaki, M. Saki, Base-promoted aminoethylation of thiols with 2-oxazolidinones: a simple synthesis of 2-aminoethyl sulfides. *Tetrahedron*, **2001**, *57*, 2115-2120.
- Sybyl X molecular modeling software packages, version 1.3; Tripos Associates, Inc.: St Louis, MO63114, **2011**.
- Sybyl molecular modeling software packages, 6.9; Tripos Associates, Inc., St Louis, MO63114, **2001**.

Supplementary Material

Supplementary data (¹H NMR and ¹³C NMR spectra) related to this article can be found at <http://XX>